Control Engineering Practice 79 (2018) 209–218

Contents lists available at ScienceDirect

Control Engineering Practice

journal homepage: www.elsevier.com/locate/conengprac

Energy-aware leader-follower tracking control for electric-powered multi-agent systems

Chuan Yan [a], Huazhen Fang [a,*], Haiyang Chao [b]

[a] Department of Mechanical Engineering, University of Kansas, Lawrence, KS, 66045, USA
[b] Department of Aerospace Engineering, University of Kansas, Lawrence, KS, 66045, USA

ARTICLE INFO

Keywords:
Multi-agent system
Battery control
Model predictive control
Distributed optimization

ABSTRACT

This paper aims to extend the operation time/range of an electric-powered multi-agent system (MAS) in leader-follower tracking tasks, through integrating battery-based energy awareness with distributed tracking control synthesis. While MASs have gained much popularity nowadays, their use and deployment are often restricted by the operation time/range, due to the limited battery capacity. In an effort to overcome such a barrier, this work proposes to leverage a battery's *rate capacity effect* to extend its runtime, which states that more energy can be drawn from the battery on less aggressive discharging rates. The battery-aware leader-follower tracking control design is then established in a model predictive control (MPC) framework, which strikes a tradeoff between tracking performance and energy consumption rates, accounts for the battery's rate capacity dynamics, and incorporates the energy and power constraints. A distributed optimization method is used to distribute the MPC across the agents of the MAS. leader-follower tracking based on the proposed distributed MPC algorithm is then evaluated through a case study and compared with an existing algorithm in the literature. The simulation results show its effectiveness in extending the operation.

1. Introduction

Recent years have witnessed a growing interest from both the academia and industry in multi-agent systems (MASs), thanks to their broad application in rescue, surveillance, search, delivery, reconnaissance and mapping missions (Lewis, Zhang, Hengster-Movric, & Das, 2014). The research progress in the past decade is represented by a wealth of literature on MAS coordinated control. However, today's electric-powered MASs can sustain only a relatively short amount of runtime for one charge, fundamentally because the current breed of battery electrochemistries are still unable to offer high energy capacity as often needed in practice. Toward achieving longer-time and wider-range MAS operation, this article for the first time studies how to extend the time/range of an MAS by taking advantage of the battery dynamics in its collaborative mission control synthesis. Specifically, the study considers an unique phenomenon inherent to batteries, namely, the rate capacity effect. Using this effect, it formulates a distributed model predictive control (MPC) approach to enable time/range-extended leader-follower tracking. The research results can find prospective use in many MAS applications and can also be generalized to deal with other types of energy-aware MAS control problems.

Literature review: An MAS is a system composed of multiple agents able to interact with each other, which allows for inter-agent connection and operation, distributed computation and control, and collective response to environment or external conditions (Ferber, 1999). With the wide application spectrum in scientific, commercial and military sectors, it has attracted research effort of both significant breadth and depth. Coordinated control design is central to the successful accomplishment of many MAS missions, having emerged as an active research field in the system and control community. In this vibrant field, problems of prime interest include group consensus (Li & Yan, 2015; Wang & Xiao, 2010; Wu & Shi, 2011; Yang, Meng, Dimarogonas, & Johansson, 2014; Yu & Wang, 2010; Yu, Yan, & Xie, 2017), swarming and flocking (Freeman, Yang, & Lynch, 2006; Olfati-Saber, 2006), formation control (Lin, Francis, & Maggiore, 2005; Mastellone, Stipanović, Graunke, Intlekofer, & Spong, 2008; Mou, Belabbas, Morse, Sun, & Anderson, 2016; Ren & Sorensen, 2008), synchronization (Dörfler, Chertkov, & Bullo, 2013; Jadbabaie, Motee, & Barahona, 2004), rendezvous (Lin, Morse, & Anderson, 2007), coverage control (Cortes, Martinez, Karatas, & Bullo, 2004; Schwager, Rus, & Slotine, 2009), containment control (Li, Ren, Liu, & Fu, 2013b; Yoo, 2013), and leader-follower tracking (Hu & Feng, 2010; Yu, Chen, & Cao, 2010). However, despite these advances, the constrained

* Corresponding author.
E-mail address: fang@ku.edu (H. Fang).

https://doi.org/10.1016/j.conengprac.2018.07.013
Received 11 March 2018; Received in revised form 25 July 2018; Accepted 29 July 2018

operation time/range of an MAS often makes it unable to meet practical needs, which is a continual challenge in this area.

Most of electric-powered MASs depend on batteries for energy storage. The most favored choice is the lithium-ion batteries (LiBs) because of their high energy density, low self-discharge and long cycle life. Yet, though considered the best among all, LiBs still do not have the energy-weight ratio high enough to support long-duration tasks due to the electrochemistry-imposed constraints. For instance, many off-the-shelf unmanned aerial vehicles can only fly for 30 min at one charge, and ground robotic vehicles mounted with LiBs of much larger capacity will see power depletion in two to three hours, according to our survey. This issue is also pointed out in a few reports, e.g., (Bertani, DeGeorge, Shang, & Aitken, 2014; Cambone, Krieg, Pace, & Linton, 2005), raising concerns about the competence of MASs for long-endurance tasks. While the materials science and electrochemistry communities are making aggressive effort to develop batteries of higher energy and power densities, real-time control of battery use offers another promising way to improve the battery performance, as demonstrated by the rich literature in the area of battery management (Rahn & Wang, 2013). A question of interest then is: can an MAS have an extended operation time and range if its system-wide coordinated control is integrated with the battery control?

With its practical significance, energy awareness is a recurring subject in control design. It is conventionally handled by formulating a cost function weighing the relative importance of the considered control objective versus that of the input energy (Chen, Hara, & Chen, 2003; Chen, Ren, Hara, & Qin, 2001) or through enforcing hard constraints on control inputs (Hu, Lin, & Chen, 2002; Su, Chen, Lam, & Lin, 2013). These studies only emphasize reducing energy consumption in the control run, regardless of the dynamic features of the power sources. When it comes to MAS control design, a large body of work likewise rarely takes energy storage into consideration and almost unanimously assumes unconstrained power availability to drive an agent, e.g., Hong, Wang, and Jiang (2013), Li, Ren, Liu, and Fu (2013a) and Yu, Yan, Xie, and Xie (2016), which though is not realistic. In reality, a battery not only has limited energy capacity and instantaneous power output but also is not an ideal linear power source as often assumed. A crucial factor contributing to a battery's nonlinear behavior is the well-known *rate capacity effect*, which states that the battery's total usable capacity goes down with an increase in discharging power (Jongerden & Haverkort, 2009). That is, the higher the discharging power, the faster the battery will be drained, or equivalently, the available capacity will decrease at a slower rate given a lower discharging power. This phenomenon implies the promise of extracting more energy from the battery to support longer-time and wider-range operation if the discharging process is controlled to be appropriately conservative yet without much compromise to the mission control objective. Similar to this notion, the literature contains several studies on communication protocol design for wireless sensor networks aware of the rate capacity effect to increase operation time, e.g. Padmanabh and Roy (2006). However, the methodologies proposed therein are not suitable here due to the difference in problem contexts and structures. Meanwhile, the ever-widening use of batteries in electrified transportation, grid and buildings has motivated a growing interest on advanced battery management algorithms, which mainly focus on state-of-charge (SoC) and state-of-health (SoH) estimation (Bartlett et al., 2016; Dey, Ayalew, & Pisu, 2015; Di Domenico, Stefanopoulou, & Fiengo, 2010; Fang, Wang, Sahinoglu, Wada, & Hara, 2014; Fang et al., 2014; Kim et al., 2015; Moura, Chaturvedi, & Krstić, 2014; Smith, Rahn, & Wang, 2010; Weng, Feng, Sun, & Peng, 2016; Zou, Manzie, Nesić, & Kallapur, 2016), charging protocol optimization (Fang, Wang, & Chen, 2017; Liu, Li, & Fathy, 2017; Suthar, Ramadesigan, De, Braatz, & Subramanian, 2014), thermal monitoring (Lin, Perez, Siegel, Stefanopoulou, Li, Anderson, Ding, & Castanier, 2013; Richardson, Ireland, & Howey, 2014), etc. Yet, they usually consider a standalone battery, without integrating the battery control with the system that it powers.

With this motivation, this paper will investigate battery-aware time/range-extended leader-follower tracking. In a leader-follower MAS, the follower agents are distributedly controlled to track the trajectory of the leader agent with real-time information exchange among them according to a communication topology. Differing from the existing work, each follower in this study will be conscious of not only the tracking objective but also the rate capacity effect intrinsic to its battery. The challenge, however, lies in how to design an effective approach to control the joint MAS-battery dynamics in a distributed manner. To overcome it, this work will consider an MPC-based design for two reasons. First, the predictive nature of MPC will allow the battery use to be planned ahead, thus enabling consciousness of battery status. Second, MPC can accommodate state and input constraints (Kerrigan, 2001; Wang, 2009), which makes it a fit for handling battery use limits. Along this line, an MPC strategy based on distributed optimization is thus developed for battery-aware tracking.

Statement of Contributions: The contributions of this work are as follows. (1) Formulation of battery-aware time/range-extended leader-follower tracking problem. It is presented in the form of receding-horizon optimization under constraints relevant to agent and nonlinear battery dynamics embodied by the battery's rate capacity effect. (2) Synthesis of a distributed MPC algorithm to address the problem. With this algorithm, each follower can use exchanged information with its neighbors to decide its control action in order to balance tracking performance and battery energy saving. The design builds on a distributed alternating direction method of multipliers (D-ADMM) method proposed in Mota, Xavier, Aguiar, and Puschel (2013). This study is the first one that we are aware of that exploits the battery's nonlinear dynamics to increase the operation time/range of an MAS.

Organization: The rest of this paper is organized as follows. Section 2 describes the problem of leader-follower tracking with an awareness of the battery's rate capacity effect. Section 3 derives the distributed MPC strategy from the perspective of distributed optimization as a solution to the considered problem. A simulation study is offered in Section 4 to illustrate the effectiveness of the proposed strategy. Finally, Section 5 gathers our concluding remarks.

Notation: The notation throughout this paper is standard. The set of real numbers is denoted by $\mathbb{R}$. The Euclidean norm of a vector is denoted as $\|\cdot\|$, and the Manhattan norm denoted as $\|\cdot\|_1$. Matrices, if their dimensions are not indicated explicitly, are assumed to be compatible in algebraic operations. Consider an MAS with one leader, which is labeled as 0, and N followers, which are labeled from 1 to N. The interaction topology among followers is modeled by an undirected graph. This graph is expressed as $\mathcal{G} = (\mathcal{V}, \mathcal{E})$, where $\mathcal{V} = \{1, 2, \dots, N\}$ is the node set and the edge set $\mathcal{E} \subseteq \mathcal{V} \times \mathcal{V}$ contains unordered pairs of nodes. A path is a sequence of connected edges in a graph. The neighbor set of agent i is denoted as $\mathcal{N}_i$, which includes all the agents in communication with it. Furthermore, combination of $\mathcal{G}$ with the leader gives a directed graph $\bar{\mathcal{G}}$ since the information exchange is one-way from the leader to the followers directly connected with it. The graph $\bar{\mathcal{G}}$ of this multi-agent system is said to be connected if at least one agent in each component of $\mathcal{G}$ is connected to the leader by a directed edge For $\bar{\mathcal{G}}$, $\bar{\mathcal{N}}_i$ represents the neighbor set of agent i. Note that $\bar{\mathcal{N}}_i = \mathcal{N}_i \cup \{0\}$ if agent i can directly communicate with the leader and $\bar{\mathcal{N}}_i = \mathcal{N}_i$ otherwise.

2. Problem formulation

This section formulates the problem of MPC-based battery-aware distributed leader-follower tracking control.

For a leader-follower MAS, the followers are expected to track the trajectory of the leader. During the tracking process, the leader and followers will maintain communication according to a pre-specified network topology to exchange their state information. Leveraging the information exchange, the followers will adjust control to themselves to achieve tracking. Suppose that a follower's dynamics is given by

$$z_i(t+1) = z_i(t) + \sigma_i u_i(t), \ i = 1, 2, \dots, N, \tag{1}$$

where $z_i \in \mathbb{R}^n$ is follower i's current state, $u_i \in \mathbb{R}^n$ the control input with $\|u_i\|_1$ assumed to be the instantaneous discharging power drawn from the onboard battery, and $\sigma_i \in \mathbb{R}^{n\times n}$ a positive diagonal matrix of constant coefficient. While the model looks simple, it is capable of describing many types of MASs and thus often used in the literature (Ren & Beard, 2008). In addition, it does not limit generalization of the following results to an MAS with higher-order dynamics. Without loss of generality, the leader's dynamics takes on a similar form:

$$z_0(t+1) = z_0(t) + \sigma_0 u_0(t), \tag{2}$$

where $z_0 \in \mathbb{R}^n$ and $u_0 \in \mathbb{R}^n$ denote the state and input of the leader, respectively, and $\sigma_0 \in \mathbb{R}^{n\times n}$ is a positive coefficient matrix. Since the leader's maneuver depends on the mission context, its control input u_0 is supposed to have been determined. Given the practical communication constraints, the leader is assumed to communicate with only part of the followers during the tracking progress.

A critical yet often neglected factor in MAS tracking control is the batteries mounted on the followers to provide power. Rather than a linear energy reservoir as widely assumed in the literature, a battery demonstrates nonlinear dynamics that can affect the amount of power and energy that it can offer. For a battery, its state is measured by the SoC, which is a percentage ratio between the available energy capacity and the maximum capacity. Denoting the SoC of follower i's battery as $x_i \in \mathbb{R}$, it is then given by

$$x_i(t) = \frac{Q_i(t)}{Q_{i,\max}} \times 100\%, \quad i = 1, 2, \dots, N,$$

where Q_i in Wh is the present capacity and $Q_{i,\max}$ is the nominal maximum capacity. Energy extraction from a battery and consequently, the change of SoC, is subjected to the rate capacity effect, which refers to the fact that the battery's usable capacity will decrease at a faster rate if the discharging power increases. This effect can be described by the well-known Peukert's law (Hausmann & Depcik, 2013):

$$C_p = I^\beta \bar{t}, \tag{3}$$

where C_p in Wh is the battery's nominal capacity calibrated at a one-ampere discharge rate, I is the actual discharging current, $\bar{t}$ is the actual time to discharge the battery, and β is the Peukert constant with $\beta > 1$. Along this line, the dynamics of SoC during discharging is governed by the following equation:

$$x_i(t+1) = x_i(t) - \alpha_i \|u_i(t)\|_1^\beta, \tag{4}$$

where $\|u_i\|_1$ is the discharging power as defined earlier, and $\alpha_i = t_s\delta_i/(3600 \cdot Q_{i,\max})$, with t_s being the sampling period in seconds and $\delta_i \geq 1$ the discharging efficiency coefficient. It should be noted that a battery's operation should be bounded for the consideration of battery safety and health (Rahn & Wang, 2013). Then to avoid overuse, a battery's SoC needs to be kept within a favorable range defined by the lower and upper limits $x_{i,\min}$ and $x_{i,\max}$, i.e.,

$$x_{i,\min} \leq x_i(t) \leq x_{i,\max}. \tag{5}$$

Meanwhile, the discharging power $\|u_i\|_1$ should also be bounded by an upper limit $u_{i,\max}$ in order to prevent life-damaging effects. Hence,

$$0 \leq \|u_i(t)\|_1 \leq u_{i,\max}. \tag{6}$$

As aforementioned, the objective of this paper is to develop a distributed control strategy for battery-aware leader-follower tracking in order to enhance the overall operation time/range. The battery awareness here mainly builds on an understanding of the rate capacity effect—if the discharging power is constrained, more energy can be extracted from the battery to support longer-duration tracking. However, a systematic control design must be performed in order to balance time/range extension and tracking performance, which will require us to answer a key question: how to jointly control the dynamics of a follower and its battery to enable energy-conscious tracking under the constraints relevant to battery operation? To address this challenge, an MPC approach is considered here. It frames the solution on the idea that the leader can inform its neighbor followers of its control decisions in an upcoming time window. Given preview of the leader's behavior, a follower can then make predictive control to extract power from its battery to track the leader. Constrained optimization can then be formulated as a result of its battery's constraints, to which MPC can well lend itself. Through appropriate design, the MPC can be distributed among the followers such that each follower can apply individual control with cognizance of the global tracking objective.

To this end, we begin with a centralized MPC for energy-conscious tracking, which is laid out as follows:

$$\min \sum_{\tau=t+1}^{t+T} \sum_{i=1}^{N} \left[q_i \sum_{j\in\mathcal{N}_i} \left\| z_i(\tau) - z_j(\tau) \right\|^2 + r_i \left(\|u_i(\tau-1)\|_1^\beta \right)^2 \right], \tag{7a}$$

$$\text{s.t. } z_i(\tau+1) = z_i(\tau) + \sigma_i u_i(\tau), \tag{7b}$$

$$z_0(\tau+1) = z_0(\tau) + \sigma_0 u_0(\tau), \tag{7c}$$

$$x_i(\tau+1) = x_i(\tau) - \alpha_i \|u_i(\tau)\|_1^\beta, \tag{7d}$$

$$x_{i,\min} \leq x_i(\tau) \leq x_{i,\max}, \tag{7e}$$

$$0 \leq \|u_i(\tau)\|_1 \leq u_{i,\max}, \tag{7f}$$

$$i = 1, 2, \dots, N, \ \tau = t, t+1, \dots, t+T-1.$$

Here, the MPC is considered for the time window from $t+1$ to $t+T$, and its cost function is quadratic and composed of two terms. The first term quantifies the squared sum of distances between follower i and its neighbors, including the leader or the other followers, and the second quadratic term expresses follower i's energy cost. Here, q_i and r_i are weighting factors to show the tradeoff between distance and energy consumption costs. The constraint (7d) serves as a predictive model able to indicate follower i's battery behavior within the window; similarly, follower i's system dynamics follows the constraint (7b). The battery's operational constraints are summarized in (7e)–(7f) as duplicates of (5)–(6). Next, we will distribute the MPC in (7) across the MAS, with the detailed development shown in Section 3.

Remark 1 (*Novelty of MPC-based leader-follower Tracking*)**.** While the problem in (7) is motivated to enable time/range-extended MAS tracking with planned battery use, it also represents the first MPC-based formulation for leader-follower tracking control to our knowledge. It is observed that this formulation brings two advantages. First, MPC would allow predictive management of the tracking mission under diverse practical operation constraints. Second, the problem formulated in (7) does not require the availability of u_0 at the end of the followers. This is a well-founded improvement to the literature, which often assumes that each follower has knowledge of the leader's instantaneous driving input u_0 even if it does not directly communicate with the leader (Hu & Feng, 2010; Yu et al., 2010).

Remark 2 (*Comparison with Saturation-based Formulation*)**.** Actuators are often subject to actuation limits, which are often modeled as control input saturation (Tarbouriech, Garcia, da Silva Jr, & Queinnec, 2011). It is understood that the saturation can bring energy saving to a certain extent. However, this mechanism is passive and relevant to local control. By contrast, the MPC-based formulation not only includes actuation limits, i.e., (7f), but also introduces active optimization between energy use and tracking performance, more advantageous from a practical perspective.

3. Distributed MPC design for energy-aware tracking

This section distributes the centralized MPC in (7a)–(7f) across the followers such that each follower will perform local control yet achieve tracking as a group. The solution will build on the D-ADMM algorithm

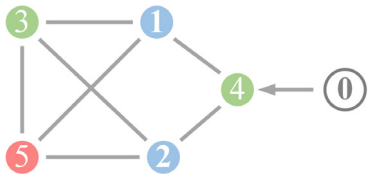

Fig. 1. Illustration of a colored MAS communication topology, with the leader numbered as 0 and the followers numbered from 1 to 5. Note that the communication from the leader to a follower is unidirectional (directed) and that the communication between followers is bidirectional (undirected). Three colors, blue, green, and red, are used to mark the undirected follower graph such that no adjacent followers share the same color, and each follower is numbered in a color-based order. Thus, $\mathcal{C}_1 = \{1,2\}$, $\mathcal{C}_2 = \{3,4\}$, and $\mathcal{C}_3 = \{5\}$. (For interpretation of the references to color in this figure legend, the reader is referred to the web version of this article.)

in Mota et al. (2013), which decomposes a centralized optimization problem into a set of distributed separable ones. This algorithm is based on the ideas that the nodes can be marked according to a coloring scheme and that local actions follow a color-based order to enable distributed optimization. To see this, let us consider the follower graph. Suppose that P colors can be used to color the followers such that no adjacent ones share the same color. The first C_1 nodes have color 1, numbered as $\{1,2,\dots,C_1\}$ and denoted as the set $\mathcal{C}_1$. Similarly, the C_p nodes have color p, collected in $\mathcal{C}_p = \{C_{p-1}+1, C_{p-1}+2, \dots, C_{p-1}+C_p\}$. It then follows that $\sum_{p=1}^{P} C_p = N$. An example is shown in Fig. 1. In what follows, we will develop the distributed MPC based on the coloring scheme.

3.1. Problem manipulation

Here, we will reformulate the centralized MPC in (7a)–(7f) into a form suitable for distributed execution. Along this line, let us first consider recasting the initial MPC problem into the consistency constraint form. Before proceeding, it is assumed that a follower can measure its own position, SoC and discharging power. Furthermore, it gathers the same information from its neighboring followers and the leader's position if the leader is a neighbor.

For follower i, its SoC variables from $t+1$ to $t+T$ can be stacked into a vector:

$$\hat{X}_i = \begin{bmatrix} \cdots & x_i(\tau) & \cdots \end{bmatrix}^\top, \tag{8}$$

for $\tau = t+1,\dots,t+T$. Furthermore, to locally paint a picture of the global network, each follower has virtual copies of state and control variables of all the other nodes in addition to its own. Hence, follower i's state variable, $\bar{z}_i$, is defined by

$$\bar{z}_i(\tau) = \begin{bmatrix} \cdots & \left(z_j^i(\tau)\right)^\top & \cdots \end{bmatrix}^\top,$$

where $j = 1,2,\dots,N$, and z_j^i represents the virtual replica of z_j in node i. Then, the predicted state vector within the window is obtained as

$$Z_i = \begin{bmatrix} \cdots & \bar{z}_i^\top(\tau) & \cdots \end{bmatrix}^\top, \tag{9}$$

for $\tau = t+1,\dots,t+T$. Thus, Z_i represents node i's replica of all the states of all the followers in the network. In order to ensure consistency among all followers, the following constraint is enforced:

$$Z_i = Z_j, \tag{10}$$

for $j \in \mathcal{N}_i$. Similarly, we define

$$\bar{u}_i(\tau) = \begin{bmatrix} \cdots & \left(u_j^i(\tau)\right)^\top & \cdots & \|u_j^i(\tau)\|_1^\beta & \cdots \end{bmatrix}^\top,$$

for $j = 1,\dots,N$, where u_j^i and $\|u_j^i\|_1^\beta$ represent the copy of u_j and $\|u_j\|_1^\beta$ stored at follower i, respectively. Note that we differentiate u_j and $\|u_j\|_1^\beta$ here, because the former is the power needed by the maneuver and the latter represents the actual power drawn due to the maneuver. The collection, $\bar{u}_j^i$ within the window, is then described as

$$U_i = \begin{bmatrix} \cdots & \bar{u}_i^\top(\tau) & \cdots \end{bmatrix}^\top, \tag{11}$$

for $\tau = t,\dots,t+T-1$. To guarantee consistency among nodes, the following condition is needed to ensure all the control copies to be equal in an edge-based way:

$$U_i = U_j,\ \forall j \in \mathcal{N}_i. \tag{12}$$

We further define $X_i = \begin{bmatrix} Z_i^\top & \hat{X}_i^\top \end{bmatrix}^\top$ and rewrite the MPC problem using all the above definitions in (7a)–(7f) into the following:

$$\min \quad \sum_{i=1}^{N} f_i(X_i, U_i), \tag{13a}$$

$$\text{s.t.} \quad A_i X_i + B_i U_i = c_i, \tag{13b}$$

$$X_i \in \mathcal{X}_i, \quad U_i \in \mathcal{U}_i, \tag{13c}$$

$$Z_i = Z_j, \ \text{for } j \in \mathcal{N}_i, \tag{13d}$$

$$U_i = U_j, \ \text{for } j \in \mathcal{N}_i, \tag{13e}$$

$$i = 1,2,\dots,N.$$

Here, f_i is the cost function posed for follower i, which is deduced from (7a), (13b) is built on a combination of predictive model in (7b) and (7d), and (13c) summarizes the state and control constraints in (7e)–(7f).

With the followers marked in different colors according to the coloring scheme introduced at the beginning of this section, the next step is to convert the problem in (13a)–(13e) and make it ready for distributed optimization. To proceed, the state and control consistency constraints in (13d) and (13e) can be rewritten as

$$\left(M^\top \otimes I_{nNT}\right)^\top \begin{bmatrix} Z_1 \\ \vdots \\ Z_N \end{bmatrix} = 0, \quad \left(M^\top \otimes I_{nNT}\right)^\top \begin{bmatrix} U_1 \\ \vdots \\ U_N \end{bmatrix} = 0, \tag{14}$$

where M is the incidence matrix of the graph of followers, $I_{nNT} \in \mathbb{R}^{nNT \times nNT}$ is the identity matrix, and $\otimes$ denotes the Kronecker product. Then, we combine the states and control inputs of the followers marked in color p into new vectors:

$$\bar{Z}_p = \begin{bmatrix} \cdots & Z_i^\top & \cdots \end{bmatrix}^\top, \quad \bar{U}_p = \begin{bmatrix} \cdots & U_i^\top & \cdots \end{bmatrix}^\top,$$

for $i \in \mathcal{C}_p$. Since the followers are numbered in the order of colors, (14) is rewritten as

$$\bar{M} \begin{bmatrix} Z_1 \\ \vdots \\ Z_N \end{bmatrix} = 0, \quad \bar{M} \begin{bmatrix} U_1 \\ \vdots \\ U_N \end{bmatrix} = 0, \tag{15}$$

where $\bar{M} = \left(M^\top \otimes I_{nNT}\right)^\top$. It is noted that $\bar{M}$ can be decomposed in a color-based manner such that (15) can be expressed equivalently as

$$\sum_{p=1}^{P} \bar{K}_p \bar{Z}_p = 0, \quad \sum_{p=1}^{P} \bar{K}_p \bar{U}_p = 0,$$

where $\bar{K}_p$ is the pth row block of $\bar{M}$. In the meantime, the states of the batteries mounted on the followers can be aggregated, one color after another:

$$\bar{X}_p = \begin{bmatrix} \cdots & \hat{X}_i^\top & \cdots \end{bmatrix}^\top,$$

for $i \in C_p$. We define $\bar{X}_p = \left[\bar{Z}_p^\top \ \bar{X}_p^\top\right]^\top$. Hence, the MPC problem in (13) can be presented in a color-separable way:

$$\min \quad \sum_{p=1}^{P} g_p\left(\bar{X}_p, \bar{U}_p\right), \tag{16a}$$

$$\text{s.t.} \quad \bar{A}_p\bar{X}_p + \bar{B}_p\bar{U}_p = \bar{c}_p, \tag{16b}$$

$$\bar{X}_p \in \bar{\chi}_p, \quad \bar{U}_p \in \bar{\mathcal{U}}_p, \quad p = 1, 2, \ldots, P, \tag{16c}$$

$$\sum_{p=1}^{P} \bar{K}_p\bar{Z}_p = 0, \tag{16d}$$

$$\sum_{p=1}^{P} \bar{K}_p\bar{U}_p = 0, \tag{16e}$$

where g_p, $\bar{\chi}_p$, $\bar{\mathcal{U}}_p$, $\bar{A}_p$, $\bar{B}_p$ and $\bar{c}_p$ can be derived from the context. Now, the original MPC problem is changed into a color-based type, which can be broken down further to achieve full distribution among individual followers.

3.2. Distributed MPC

Here, we develop distributed MPC based on the problem in (16), leveraging the D-ADMM algorithm in Mota et al. (2013). To begin with, the augmented Lagrangian function for (16) is defined as

$$\begin{aligned} L = \sum_{p=1}^{P}\Big[g_p\left(\bar{X}_p, \bar{U}_p\right) + \lambda_p^\top\left(\bar{A}_p\bar{X}_p + \bar{B}_p\bar{U}_p - \bar{c}_p\right) + \varphi^\top\bar{K}_p\bar{Z}_p + \eta^\top\bar{K}_p\bar{U}_p \\ + \frac{\rho_1}{2}\left\|\bar{A}_p\bar{X}_p + \bar{B}_p\bar{U}_p - \bar{c}_p\right\|^2\Big] + \frac{\rho_2}{2}\left\|\sum_{p=1}^{P}\bar{K}_p\bar{Z}_p\right\|^2 + \frac{\rho_3}{2}\left\|\sum_{p=1}^{P}\bar{K}_p\bar{U}_p\right\|^2, \end{aligned} \tag{17}$$

where $\lambda_p > 0$, φ and η are dual variables, and ρ_1, ρ_2 and ρ_3 are positive penalty parameters. Using the alternating direction method of multipliers (ADMM), minimizing $\bar{X}_p$ and $\bar{U}_p$ can be achieved through the following iterative procedure:

$$\bar{X}_p^{k+1} = \underset{\bar{U}_p\in\bar{\mathcal{U}}_p}{\arg\min} L\left(\bar{X}_1^{k+1}, \bar{U}_1^{k+1}, \ldots, \bar{X}_p, \bar{U}_p^k, \ldots, \bar{X}_P^k, \bar{U}_P^k; \lambda_p^k, \varphi^k, \eta^k\right), \tag{18}$$

$$\bar{U}_p^{k+1} = \underset{\bar{X}_p\in\bar{\chi}_p}{\arg\min} L\left(\bar{X}_1^{k+1}, \bar{U}_1^{k+1}, \ldots, \bar{X}_p^{k+1}, \bar{U}_p, \ldots, \bar{X}_P^k, \bar{U}_P^k; \lambda_p^k, \varphi^k, \eta^k\right), \tag{19}$$

$$\lambda_p^{k+1} = \lambda_p^k + \rho_1\left(\bar{A}_p\bar{X}_p^{k+1} + \bar{B}_p\bar{U}_p^{k+1} - \bar{c}_p\right), \tag{20}$$

$$\varphi^{k+1} = \varphi^k + \rho_2\sum_{p=1}^{P}\bar{K}_p\bar{Z}_p^{k+1}, \tag{21}$$

$$\eta^{k+1} = \eta^k + \rho_3\sum_{p=1}^{P}\bar{K}_p\bar{U}_p^{k+1}, \tag{22}$$

where k is the iteration counter.

It is seen that (18) can be explicitly given as

$$\begin{aligned} \bar{X}_p^{k+1} &= \underset{\bar{X}_p\in\bar{\chi}_p g_p}{\arg\min}\left(\bar{X}_p, \bar{U}_p^k\right) \\ &\quad + \left(\lambda_p^k\right)^\top\left(\bar{A}_p\bar{X}_p + \bar{B}_p\bar{U}_p^k - \bar{c}_p\right) + \left(\varphi^k\right)^\top\bar{K}_p\bar{Z}_p + \left(\eta^k\right)^\top\bar{K}_p\bar{U}_p^k \\ &\quad + \frac{\rho_1}{2}\left\|\bar{A}_p\bar{X}_p + \bar{B}_p\bar{U}_p^k - \bar{c}_p\right\|^2 \\ &\quad + \frac{\rho_2}{2}\left\|\bar{K}_p\bar{Z}_p + \sum_{i=1,\ldots,P,\ i\neq p}\bar{K}_i\bar{Z}_i^k\right\|^2 + \frac{\rho_3}{2}\left\|\sum_{i=1}^{P}\bar{K}_i\bar{U}_i\right\|^2 \\ &= \underset{\bar{X}_p\in\bar{\chi}_p g_p}{\arg\min}\left(\bar{X}_p, \bar{U}_p^k\right) + \left(\lambda_p^k\right)^\top\left(\bar{A}_p\bar{X}_p + \bar{B}_p\bar{U}_p^k - \bar{c}_p\right) \\ &\quad + \left(\varphi^k\right)^\top\bar{K}_p\bar{Z}_p \\ &\quad + \frac{\rho_1}{2}\left\|\bar{A}_p\bar{X}_p + \bar{B}_p\bar{U}_p^k - \bar{c}_p\right\|^2 + \frac{\rho_2}{2}\left\|\bar{K}_p\bar{Z}_p + \sum_{i=1,\ldots,P,\ i\neq p}\bar{K}_i\bar{Z}_i^k\right\|^2. \end{aligned} \tag{23}$$

From above, the first three terms of the right-hand side of (23) are each a linear combination relative to the individual color-p followers. Further, the last term in (23) can be expressed as

$$\begin{aligned} \left\|\bar{K}_p\bar{Z}_p + \sum_{i=1,\ldots,P,\ i\neq p}\bar{K}_i\bar{Z}_i^k\right\|^2 &= \bar{Z}_p^\top\bar{K}_p^\top\bar{K}_p\bar{Z}_p + 2\bar{Z}_p^\top\bar{K}_p^\top\sum_{i=1,\ldots,P,\ i\neq p}\bar{K}_i\bar{Z}_i^k \\ &\quad + \left\|\sum_{i=1,\ldots,P,\ i\neq p}\bar{K}_i\bar{Z}_i^k\right\|^2. \end{aligned} \tag{24}$$

Since color-p nodes do not connect to each other, the term $\bar{K}_p^\top\bar{K}_p$ turns out to be a diagonal matrix with the diagonal elements being the degree of respective node, i.e.,

$$\bar{Z}_p^\top\bar{K}_p^\top\bar{K}_p\bar{Z}_p = \sum_{i\in C_p} D_i\left\|\bar{Z}_i\right\|^2, \tag{25}$$

where D_i is the degree of node i. Meanwhile, $\bar{K}_p^\top\bar{K}_i = -I_{nNT}$ for $p \neq i$, and we have

$$\bar{Z}_p^\top\bar{K}_p^\top\sum_{i=1,\ldots,P,\ i\neq p}\bar{K}_i\bar{Z}_i^k = -\sum_{i\in C_p}\sum_{j\in\mathcal{N}_i} Z_i^\top Z_j^k. \tag{26}$$

With (24)–(26), (23) can be simplified as

$$\begin{aligned} \bar{X}_p^{k+1} =& \underset{\bar{X}_p\in\bar{\chi}_p g_p}{\arg\min}\left(\bar{X}_p, \bar{U}_p^k\right) + \left(\lambda_p^k\right)^\top\left(\bar{A}_p\bar{X}_p + \bar{B}_p\bar{U}_p^k - \bar{c}_p\right) \\ &+ \frac{\rho_1}{2}\left\|\bar{A}_p\bar{X}_p + \bar{B}_p\bar{U}_p^k - \bar{c}_p\right\|^2 \\ &+ \left(\mu_i^k - \rho_2\sum_{j\in\mathcal{N}_i} Z_j^k\right)^\top Z_i + \frac{\rho_2 D_i}{2}\|Z_i\|^2, \end{aligned} \tag{27}$$

where $\mu_i^k = \sum_{j\in\mathcal{N}_i}\mathrm{sign}(j-i)\cdot\varphi_{ij}^k$. We define an auxiliary dual variable $\phi_i^k = \mu_i^k - \rho_2\sum_{j\in\mathcal{N}_i,\ j<i} Z_j^{k+1} - \rho_2\sum_{j\in\mathcal{N}_i,\ j>i} Z_j^k$. The above equation, as a linear combination of Lagrangians of the color-p nodes, can then be split with respect to X_i for $i \in C_p$, i.e.,

$$\begin{aligned} X_i^{k+1} &= \underset{X_i\in\mathcal{X}_i}{\arg\min} f_i\left(X_i, U_i^k\right) + \left(\gamma_i^k\right)^\top\left(A_iX_i + B_iU_i^k - c_i\right) \\ &\quad + \frac{\rho_1}{2}\left\|A_iX_i + B_iU_i^k - c_i\right\|^2 + \left(\phi_i^k\right)^\top Z_i + \frac{\rho_2 D_i}{2}\|Z_i\|^2, \end{aligned}$$

where $i \in C_p$ and γ_i is the dual variable at the local node i, i.e.,

$$\lambda_p = \begin{bmatrix}\cdots & \gamma_i^\top & \cdots\end{bmatrix}^\top.$$

Now we consider the iterative update of $\bar{U}_p$ in (19), which can be expressed as

$$\begin{aligned} \bar{U}_p^{k+1} &= \underset{\bar{U}_p\in\bar{\mathcal{U}}_p}{\arg\min} g_p\left(\bar{X}_p^{k+1}, \bar{U}_p\right) + \left(\lambda_p^k\right)^\top\left(\bar{A}_p\bar{X}_p^{k+1} + \bar{B}_p\bar{U}_p - \bar{c}_p\right) \\ &\quad + \left(\eta^k\right)^\top\bar{K}_p\bar{U}_p \\ &\quad + \frac{\rho_1}{2}\left\|\bar{A}_p\bar{X}_p^{k+1} + \bar{B}_p\bar{U}_p - \bar{c}_p\right\|^2 + \frac{\rho_3}{2}\left\|\bar{K}_p\bar{U}_p + \sum_{i=1,\ldots,P,\ i\neq p}\bar{K}_i\bar{U}_i^k\right\|^2. \end{aligned} \tag{28}$$

Following lines similar to the above, (28) is also separable with respect to U_i, which results in

$$\begin{aligned} U_i^{k+1} &= \underset{U_i\in\mathcal{U}_i}{\arg\min} f_i\left(X_i^{k+1}, U_i\right) + \left(\gamma_i^k\right)^\top\left(A_iX_i^{k+1} + B_iU_i - c_i\right) \\ &\quad + \frac{\rho_1}{2}\left\|A_iX_i^{k+1} + B_iU_i - c_i\right\|^2 + \left(\xi_i^k\right)^\top U_i + \frac{\rho_3 D_i}{2}\|U_i\|^2, \end{aligned} \tag{29}$$

where $\xi_i^k = \psi_i^k - \rho_3\sum_{j\in\mathcal{N}_i,\ j<i} U_j^{k+1} - \rho_3\sum_{j\in\mathcal{N}_i,\ j>i} U_j^k$ and $\psi_i^k = \sum_{j\in\mathcal{N}_i}\mathrm{sign}(j-i)\cdot\eta_{ij}^k$.

After the updates of X_i and U_i at follower i, the dual variable γ_i can be updated as

$$\gamma_i^{k+1} = \rho_1\left(A_iX_i^{k+1} + B_iU_i^{k+1} - c_i\right).$$

Table 1
Distributed MPC algorithm for battery-aware leader–follower tracking.

initialize: set $X_i^1 = 0, U_i^1 = 0, \gamma_i^1 = 0, \mu_i^1 = 0, \psi_i^1 = 0$
repeat
$k \leftarrow k+1$
for $p = 1, 2, \cdots, P$ **do**
for $i \in C_p$ or $i = C_{p-1}+1, \cdots, C_{p-1}+C_p$ **do**
do

$$\phi_i^k = \mu_i^k - \rho_2 \sum_{j\in\mathcal{N}_i, j<i} Z_j^{k+1} - \rho_2 \sum_{j\in\mathcal{N}_i, j>i} Z_j^k$$

find

$$X_i^{k+1} = \arg\min_{X_i\in\mathcal{X}_i} f_i\left(X_i, U_i^k\right) + \left(\gamma_i^k\right)^\top \left(A_i X_i + B_i U_i^k - c_i\right) + \frac{\rho_1}{2}\left\|A_i X_i + B_i U_i^k - c_i\right\|^2 + \left(\phi_i^k\right)^\top Z_i + \frac{\rho_2 D_i}{2}\|Z_i\|^2$$

do

$$\xi_i^k = \psi_i^k - \rho_3 \sum_{j\in\mathcal{N}_i, j<i} U_j^{k+1} - \rho_3 \sum_{j\in\mathcal{N}_i, j>i} U_j^k$$

find

$$U_i^{k+1} = \arg\min_{U_i\in\mathcal{U}_i} f_i\left(X_i^{k+1}, U_i\right) + \left(\gamma_i^k\right)^\top \left(A_i X_i^{k+1} + B_i U_i - c_i\right) + \frac{\rho_1}{2}\left\|A_i X_i^{k+1} + B_i U_i - c_i\right\|^2 + \left(\xi_i^k\right)^\top U_i + \frac{\rho_3 D_i}{2}\|U_i\|^2$$

do

$$\gamma_i^{k+1} = \rho_1\left(A_i X_i^{k+1} + B_i U_i^{k+1} - c_i\right)$$

end for
end for
for $i = 1, 2\cdots, N$ **do**
do

$$\mu_i^{k+1} = \mu_i^k + \rho_2 \sum_{j\in\mathcal{N}_i}\left(Z_i^{k+1} - Z_j^{k+1}\right)$$

$$\psi_i^{k+1} = \psi_i^k + \rho_3 \sum_{j\in\mathcal{N}_i}\left(U_i^{k+1} - U_j^{k+1}\right)$$

end for
until certain pre-set stopping criterion is met

On the completion of updating X_i, U_i and γ_i for all the nodes, we can update μ_i and ψ_i

$$\mu_i^{k+1} = \mu_i^k + \rho_2 \sum_{j\in\mathcal{N}_i}\left(Z_i^{k+1} - Z_j^{k+1}\right),$$

$$\psi_i^{k+1} = \psi_i^k + \rho_3 \sum_{j\in\mathcal{N}_i}\left(U_i^{k+1} - U_j^{k+1}\right),$$

where $i = 1, 2, \ldots, N$.

Up to this point, we have obtained a distributed MPC algorithm, which is summarized in Table 1. This algorithm fully distributes the original centralized MPC among the followers. As a result, a follower can learn about its neighbors' states and make individual control decision to minimize a global cost function collectively. In this MPC setting, the follower takes into account its own local power consumption constraints and the global objective that weighs the overall energy cost against tracking performance. This will bring the advantage of drawing power at a slower rate from the battery, which implies that more energy can be drawn due to the rate capacity effect. Then, the battery runtime and MAS operation range are both extended.

Remark 3 (*Stability, Feasibility and Convergence*). Stability and feasibility analysis have been studied in the literature for a few classes of MPC problems. The proofs are often based on prediction horizons of an infinite length or well-designed terminal costs (Zheng, Negenborn, & Lodewijks, 2017). Such conditions are not appropriate for leader-follower tracking because of the versatile situations in a tracking process. Hence, what is of more interest here is whether the solution of the distributed MPC can converge to the optimal solution of the original centralized MPC. Here, the convergence is ensured. It is proven in Mota et al. (2013) that D-ADMM algorithm will converge to optimal solution if the cost function is strongly convex and the network is connected, and these conditions are satisfied here according to (7).

Remark 4 (*Extensions of the Proposed Work*). This work, for the first time, develops an approach for distributed leader-follower tracking control with a consciousness of battery use, which can increase operation time/range. Building upon this work, further extensions can be made to enhance the approach design and performance. A first one is computationally faster distributed control. The proposed distributed MPC can be executed using different methods and solvers. One option is the active set algorithm, which would eventually solves a quadratic programming. This involves polynomial computational complexity and is suitable only for a small- to medium-size network. If an MAS includes many agents, computational efficiency must be factored into the control design procedure. Second, this work does not consider time delays though the algorithm is supposed to have certain robustness to this issue. Large time delays, however, can seriously degrade the algorithm's performance and convergence. This would necessitate a modification of the proposed design that accounts for time delays. In this regard, one can find useful inspirations from a wealth literature about time-delay-robust distributed optimization and MPC, e.g., Hatanaka, Chopra, Ishizaki, and Li (2018) and Li and Shi (2013, 2017), to name just several. Finally, the proposed results can be readily generalized to an MAS with higher-order and even nonlinear dynamics, due to the wide applicability of the D-ADMM algorithm by design. The generalization can be performed along lines similar to the above development.

4. Numerical study

In this section, we provide an illustrative example to verify the effectiveness of the proposed distributed MPC algorithm. Consider a

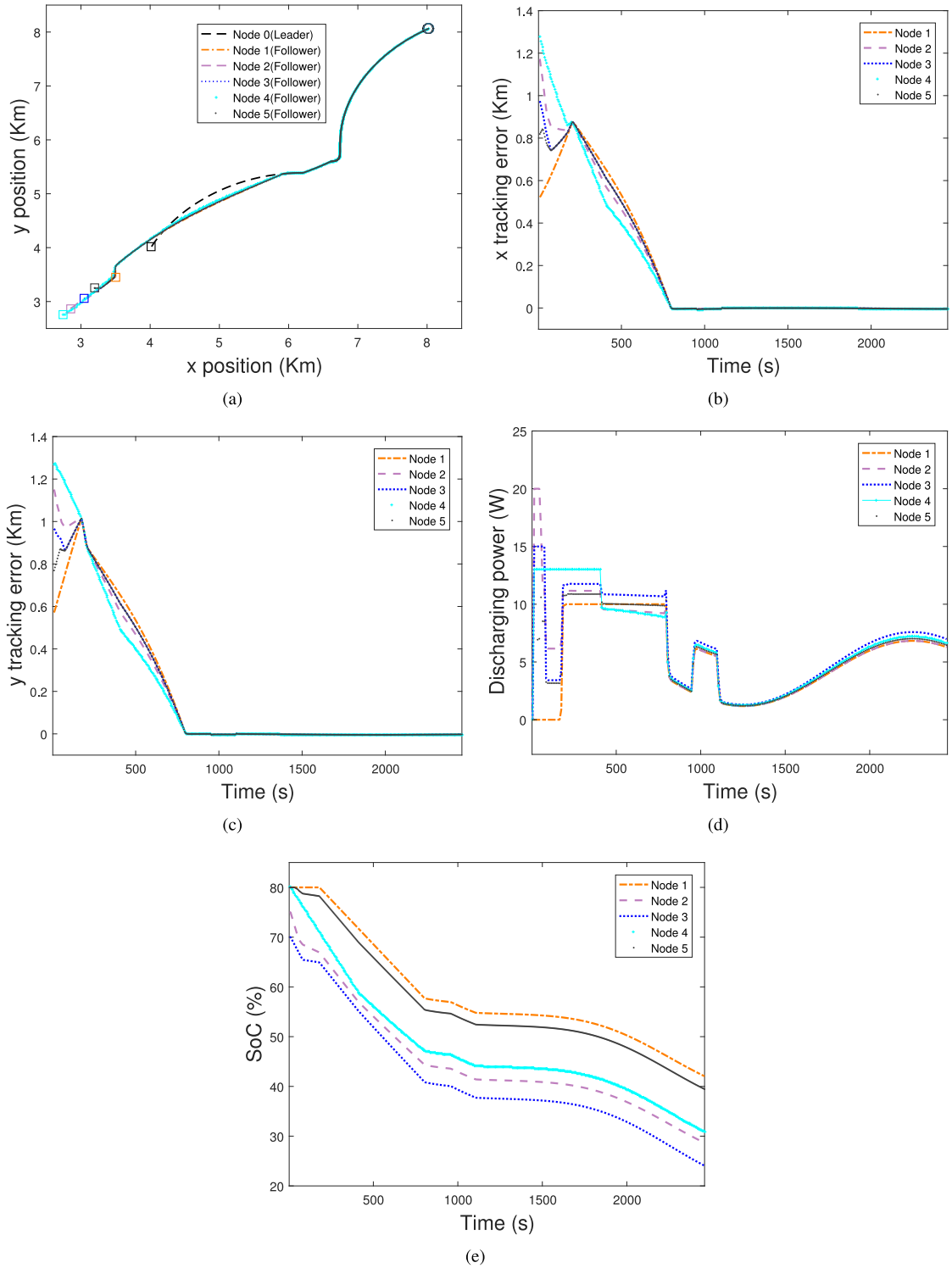

Fig. 2. Leader–follower tracking using the proposed distributed MPC algorithm: (a) state trajectory in the MAS; (b) x tracking error in the MAS; (c) y tracking error in the MAS; (d) power discharging; (e) evolution of SoC.

battery-powered MAS consisting of one leader and five followers. The communication topology among them is shown in Fig. 1, in which node 0 is the leader, and nodes 1 to 5 are followers. The leader will only send state updates to follower 1, and the followers maintain bidirectional communication with their neighbors.

Suppose that the ith agent's dynamics can be described by a model used in Ren and Sorensen (2008) and applicable to many robotic vehicles. Let (r_{xi}, r_{yi}), θ_i, and (v_i, ω_i) denote its Cartesian position, orientation, and linear and angular velocity, respectively. The kinematic equations are given by

$$\dot{r}_{xi} = v_i \cos(\theta_i), \tag{30a}$$

$$\dot{r}_{yi} = v_i \sin(\theta_i), \tag{30b}$$

$$\dot{\theta}_i = \omega_i. \tag{30c}$$

We apply feedback linearization to (30) around a fixed point denoted as (x_i, y_i), where $x_i = r_{xi} + d_i \cos(\theta_i)$ and $y_i = r_{yi} + d_i \sin(\theta_i)$ with $d_i = 0.15$ m.

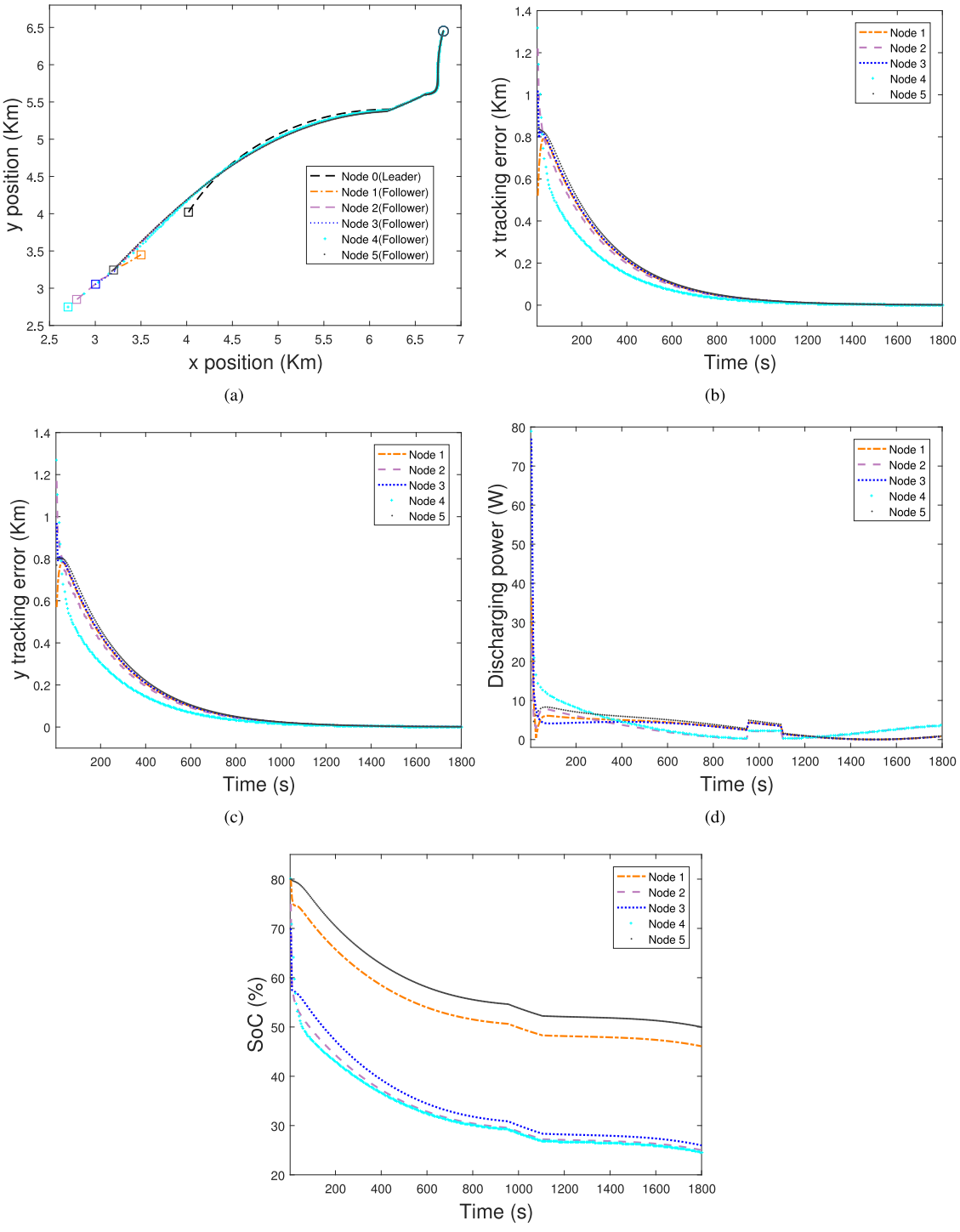

Fig. 3. Leader–follower tracking using the distributed control algorithm in Yu et al. (2016): (a) state trajectory in the MAS; (b) x tracking error in the MAS; (c) y tracking error in the MAS; (d) power discharging; (e) evolution of SoC.

Given

$$\begin{bmatrix} v_i \\ \omega_i \end{bmatrix} = \begin{bmatrix} \cos(\theta_i) & \sin(\theta_i) \\ -\frac{1}{d_i}\sin(\theta_i) & \frac{1}{d_i}\cos(\theta_i) \end{bmatrix} \begin{bmatrix} u_{xi} \\ u_{yi} \end{bmatrix},$$

it follows that

$$\begin{bmatrix} \dot{x}_i \\ \dot{y}_i \end{bmatrix} = \begin{bmatrix} u_{xi} \\ u_{yi} \end{bmatrix}.$$

The initial states of the leader and followers are set to be $(4.02, 4.02)$, $(3.5, 3.45)$, $(2.8, 2.85)$, $(3, 3.05)$, $(2.7, 2.75)$ and $(3.2, 3.25)$. For each agent, it is assumed that $\sigma_i = 0.03 I_2$ for $i = 0, 1, \ldots, N$. The followers' batteries have different capacities, SoC and instantaneous power constraints, and initial states, which are summarized in Table 2. The battery specifics are selected according to some commercially available robotic vehicles used for lab-scale MASs. We assume that the maneuver input profile applied

Table 2
Followers' battery parameters and operating bounds.

Follower	$Q_{i,\max}$ (Wh)	$x_{i,\min}$ (%)	$x_{i,\max}$ (%)	$x_i(0)$ (%)	$u_{i,\max}$ (W)
1	36	20	90	80	10
2	36	25	80	75	20
3	40	24	90	70	15
4	38	24	85	80	13
3	37	25	80	80	17

to the leader is given as

$$u_0(t) = \begin{cases} \begin{bmatrix} 5\sin(0.005\pi t) + 5 \\ 5\cos(0.005\pi t) + 5 \end{bmatrix} \text{(W)}, & 0 \le t \le 950 \text{ s}, \\ \begin{bmatrix} 5\sin(0.005\pi t) + 10 \\ 5\cos(0.005\pi t) + 10 \end{bmatrix} \text{(W)}, & 950 \text{ s} < t \le 1,100 \text{ s}, \\ \begin{bmatrix} 5\sin(0.005\pi t) + 5 \\ 5\cos(0.005\pi t) + 5 \end{bmatrix} \text{(W)}, & t > 1,100 \text{ s}. \end{cases}$$

Here, $u_0(t)$ is designed to include both aggressive and non-aggressive maneuvers from a realistic perspective. The sampling period $t_s = 5$ s, and the window length $T = 3$, equivalent to fifteen-second or three-step-ahead prediction. For the batteries, the discharging efficiency coefficients are given as $\delta_i = 1$ for each follower i for simplicity. The Peukert constant is set as $\beta = \frac{5}{3}$. For the cost function in MPC, the weight coefficients are $q_i = 1$ and $r_i = 1$ for each follower i, and the penalty parameters involved in the distributed algorithm are set as $\rho_1 = 1$, $\rho_2 = 1$ and $\rho_3 = 1$.

The distributed MPC algorithm in Table 1 is applied to the above MAS for leader-follower tracking, with the simulation results shown in Fig. 2. To make a comparison, a tracking control strategy proposed in Yu et al. (2016) is also applied to the MAS. The results obtained are illustrated in Fig. 3.

Fig. 2(a) shows the trajectories of the leader and the followers using distributed MPC. It is seen that all the followers make an effort to track the leader. However, the followers are not rushing to approach the leader as soon as possible—there is an obvious tracking error maintained before the first about 5.8 km in x-axis direction. This is because the followers are subject to power constraints and seek energy-aware tracking, refraining from fast maneuvers at fast energy consumption. After catching up with the leader, the followers then keep more accurate tracking. The evolutions of the position tracking errors are further shown in Fig. 2(b) and 2(c). From these two figures, the tracking errors of all the followers relative to the leader gradually decrease to zero at around 800 s in both x- and y-axis directions. Looking at the discharging profiles in Fig. 2(d), one can see that the followers adjust their individual power supply while obeying their own operation limits. In particular, the discharging power of followers 1 and 5 is zero at the first few seconds, which can be considered as "waiting" for followers 2, 3 and 4. They then jump to the upper power limit to start tracking the leader. The followers see their discharging power running at different levels due to their own battery constraints. At about the 800th s, the discharging power of all the followers drops because the followers catch up with the leader. After sometime, the followers increase the discharging power again as the leader begins large maneuvers. In the final stage, the followers continue to adjust the discharging power to maintain tracking of the leader. The SoC profiles of the followers are shown in Fig. 2(e). It is observed that follower 3 is the first to see battery depletion, which ends the tracking process.

Let us now consider the case when the method in Yu et al. (2016) is used. Figs. 3(a) and 3(b) and 3(c) illustrate an exponential convergence of tracking, due to the assumed unlimited instantaneous power available to each follower. Associated with this, the discharging profiles in Fig. 3(d) show that considerable power is applied in the initial stage, which leads to fast tracking. However, this comes at the expense of significantly short runtime. Fig. 3(e) demonstrates the SoC decreasing more rapidly, and when follower 4 reaches its lower SoC limit, the operation time lasts for nearly only 1800 s. By comparison, the total operation time of the MAS under the distributed MPC strategy is around 2460 s, representing an improvement of 37%. With the time extension, the range of the MAS is also increased. According to Figs. 2(a) and 3(a), the leader's cruise distance reaches 5.68 km from 3.70 km, provided that all the followers can keep tracking. This counts as an increase of 53% in traveling distance. These results demonstrate the effectiveness of the proposed approach. It should also be pointed out that the time/range extension can be made more significant if one imposes stricter constraints on the power consumption limits.

5. Conclusion

This paper considers energy-aware time/range-extended cooperative tracking. Electric-powered MASs nowadays often face limited energy budget and consequently, limited operation time/range, due to the limitations imposed by the onboard batteries. It thus becomes a pressing need to extract the maximum energy from the batteries to increase the time/range of an MAS, which, however, remains unexplored thus far. Motivated by this need, this paper investigates the leader-follower tracking problem and proposes to integrate the MAS dynamics with battery dynamics. In this regard, the promising opportunity is identified that a battery's rate capacity effect can be exploited to help draw more energy from the battery. Then, an MPC problem is formulated to deal with MAS leader-follower tracking with a cognizance of the batteries' rate capacity dynamics and power/energy constraints. It is solved by a distributed optimization strategy, which leads to a distributed MPC algorithm. Simulation results show its considerable effectiveness in extending the operation time/range of an MAS in comparison with an existing algorithm.

References

Bartlett, A., Marcicki, J., Onori, S., Rizzoni, G., Yang, X. G., & Miller, T. (2016). Electrochemical model-based state of charge and capacity estimation for a composite electrode lithium-ion battery. *IEEE Transactions on Control Systems Technology*, *24*(2), 384–399.

Bertani, A., DeGeorge, Z., Shang, Y., & Aitken, E. (2014). 2014 intelligent ground vehicle competition, Tech. rep.

Cambone, S. A., Krieg, K. J., Pace, P., & Linton, W. (2005). Unmanned aircraft systems roadmap 2005-2030. *Office of the Secretary of Defense*, *8*, 4–15.

Chen, J., Hara, S., & Chen, G. (2003). Best tracking and regulation performance under control energy constraint. *IEEE Transactions on Automatic Control*, *48*(8), 1320–1336.

Chen, J., Ren, Z., Hara, S., & Qin, L. (2001). Optimal tracking performance: preview control and exponential signals. *IEEE Transactions on Automatic Control*, *46*(10), 1647–1653.

Cortes, J., Martinez, S., Karatas, T., & Bullo, F. (2004). Coverage control for mobile sensing networks. *IEEE Transactions on Robotics and Automation*, *20*(2), 243–255.

Dey, S., Ayalew, B., & Pisu, P. (2015). Nonlinear robust observers for state-of-charge estimation of lithium-ion cells based on a reduced electrochemical model. *IEEE Transactions on Control Systems Technology*, *23*(5), 1935–1942.

Di Domenico, D., Stefanopoulou, A., & Fiengo, G. (2010). Lithium-ion battery state of charge and critical surface charge estimation using an electrochemical model-based extended Kalman filter. *Journal of Dynamic Systems, Measurement, and Control*, *132*(6), 061302.

Dörfler, F., Chertkov, M., & Bullo, F. (2013). Synchronization in complex oscillator networks and smart grids. *Proceedings of the National Academy of Sciences*, *110*(6), 2005–2010.

Fang, H., Wang, Y., & Chen, J. (2017). Health-aware and user-involved battery charging management for electric vehicles: Linear quadratic strategies. *IEEE Transactions on Control Systems Technology*, *25*(3), 911–923.

Fang, H., Wang, Y., Sahinoglu, Z., Wada, T., & Hara, S. (2014). State of charge estimation for lithium-ion batteries: An adaptive approach. *Control Engineering Practice*, *25*, 45–54.

Fang, H., Zhao, X., Wang, Y., Sahinoglu, Z., Wada, T., Hara, S., et al. (2014). Improved adaptive state-of-charge estimation for batteries using a multi-model approach. *Journal of Power Sources*, *254*, 258–267.

Ferber, J. (1999). *Multi-agent systems: An introduction to distributed artificial intelligence*. Addison-Wesley Reading.

Freeman, R. A., Yang, P., & Lynch, K. M. (2006). Distributed estimation and control of swarm formation statistics. In *American control conference, 2006*. IEEE.

Hatanaka, T., Chopra, N., Ishizaki, T., & Li, N. (2018). Passivity-based distributed optimization with communication delays using PI consensus algorithm. *IEEE Transactions on Automatic Control* (in press).

Hausmann, A., & Depcik, C. (2013). Expanding the Peukert equation for battery capacity modeling through inclusion of a temperature dependency. *Journal of Power Sources*, *235*, 148–158.

Hong, Y., Wang, X., & Jiang, Z. P. (2013). Distributed output regulation of leader-follower multi-agent systems. *International Journal of Robust and Nonlinear Control*, *23*(1), 48–66.

Hu, J., & Feng, G. (2010). Distributed tracking control of leader-follower multi-agent systems under noisy measurement. *Automatica*, *46*(8), 1382–1387.

Hu, T., Lin, Z., & Chen, B. M. (2002). An analysis and design method for linear systems subject to actuator saturation and disturbance. *Automatica*, *38*(2), 351–359.

Jadbabaie, A., Motee, N., & Barahona, M. (2004). On the stability of the Kuramoto model of coupled nonlinear oscillators. In *American control conference, 2004. proceedings of the 2004, Vol. 5* (pp. 4296–4301). IEEE.

Jongerden, M. R., & Haverkort, B. R. (2009). Which battery model to use? *IET software*, *3*(6), 445–457.

Kerrigan, E. C. (2001). Robust constraint satisfaction: invariant sets and predictive control, University of Cambridge.

Kim, T., Wang, Y., Fang, H., Sahinoglu, Z., Wada, T., Hara, S., et al. (2015). Model-based condition monitoring for lithium-ion batteries. *Journal of Power Sources*, *295*, 16–27.

Lewis, F. L., Zhang, H., Hengster-Movric, K., & Das, A. (2014). *Cooperative control of multi-agent systems*. Springer-Verlag London.

Li, Z., Ren, W., Liu, X., & Fu, M. (2013a). Consensus of multi-agent systems with general linear and Lipschitz nonlinear dynamics using distributed adaptive protocols. *IEEE Transactions on Automatic Control*, *58*(7), 1786–1791.

Li, Z., Ren, W., Liu, X., & Fu, M. (2013b). Distributed containment control of multi-agent systems with general linear dynamics in the presence of multiple leaders. *International Journal of Robust and Nonlinear Control*, *23*(5), 534–547.

Li, H., & Shi, Y. (2013). Distributed model predictive control of constrained nonlinear systems with communication delays. *Systems & Control Letters*, *62*(10), 819–826.

Li, H., & Shi, Y. (2017). *Robust receding horizon control for networked and distributed nonlinear systems*. Springer International Publishing.

Li, H., & Yan, W. (2015). Receding horizon control based consensus scheme in general linear multi-agent systems. *Automatica*, *56*, 12–18.

Lin, Z., Francis, B., & Maggiore, M. (2005). Necessary and sufficient graphical conditions for formation control of unicycles. *IEEE Transactions on Automatic Control*, *50*(1), 121–127.

Lin, J., Morse, A. S., & Anderson, B. D. (2007). The multi-agent rendezvous problem. Part 2: The asynchronous case. *SIAM Journal on Control and Optimization*, *46*(6), 2120–2147.

Lin, X., Perez, H. E., Siegel, J. B., Stefanopoulou, A. G., Li, Y., Anderson, R. D., et al. (2013). Online parameterization of lumped thermal dynamics in cylindrical lithium ion batteries for core temperature estimation and health monitoring. *IEEE Transactions on Control Systems Technology*, *21*(5), 1745–1755.

Liu, J., Li, G., & Fathy, H. K. (2017). An extended differential flatness approach for the health-conscious nonlinear model predictive control of lithium-ion batteries. *IEEE Transactions on Control Systems Technology*, *25*(5), 1882–1889.

Mastellone, S., Stipanović, D. M., Graunke, C. R., Intlekofer, K. A., & Spong, M. W. (2008). Formation control and collision avoidance for multi-agent non-holonomic systems: Theory and experiments. *International Journal of Robotics Research*, *27*(1), 107–126.

Mota, J. F., Xavier, J. M., Aguiar, P. M., & Puschel, M. (2013). D-ADMM: A communication-efficient distributed algorithm for separable optimization. *IEEE Transactions on Signal Processing*, *61*(10), 2718–2723.

Mou, S., Belabbas, M. A., Morse, A. S., Sun, Z., & Anderson, B. D. O. (2016). Undirected rigid formations are problematic. *IEEE Transactions on Automatic Control*, *61*(10), 2821–2836.

Moura, S. J., Chaturvedi, N. A., & Krstić, M. (2014). Adaptive partial differential equation observer for battery state-of-charge/state-of-health estimation via an electrochemical model. *Journal of Dynamic Systems, Measurement, and Control*, *136*(1), 011015.

Olfati-Saber, R. (2006). Flocking for multi-agent dynamic systems: Algorithms and theory. *IEEE Transactions on Automatic Control*, *51*(3), 401–420.

Padmanabh, K., & Roy, R. (2006). Maximum lifetime routing in wireless sensor network by minimizing rate capacity effect. In *Parallel processing workshops, 2006. ICPP 2006 workshops. 2006 international conference on*. IEEE.

Rahn, C. D., & Wang, C. Y. (2013). *Battery systems engineering*. John Wiley & Sons.

Ren, W., & Beard, R. (2008). *Distributed consensus in multivehicle cooperative control: Theory and applications*. Springer-Verlag London.

Ren, W., & Sorensen, N. (2008). Distributed coordination architecture for multi-robot formation control. *Robotics and Autonomous Systems*, *56*(4), 324–333.

Richardson, R. R., Ireland, P. T., & Howey, D. A. (2014). Battery internal temperature estimation by combined impedance and surface temperature measurement. *Journal of Power Sources*, *265*, 254–261.

Schwager, M., Rus, D., & Slotine, J. J. (2009). Decentralized, adaptive coverage control for networked robots. *International Journal of Robotics Research*, *28*(3), 357–375.

Smith, K. A., Rahn, C. D., & Wang, C. Y. (2010). Model-based electrochemical estimation and constraint management for pulse operation of lithium ion batteries. *IEEE Transactions on Control Systems Technology*, *18*(3), 654–663.

Su, H., Chen, M. Z., Lam, J., & Lin, Z. (2013). Semi-global leader-following consensus of linear multi-agent systems with input saturation via low gain feedback. *IEEE Transactions on Circuits and Systems. I. Regular Papers*, *60*(7), 1881–1889.

Suthar, B., Ramadesigan, V., De, S., Braatz, R. D., & Subramanian, V. R. (2014). Optimal charging profiles for mechanically constrained lithium-ion batteries. *Physical Chemistry Chemical Physics*, *16*(1), 277–287.

Tarbouriech, S., Garcia, G., da Silva Jr, J. M. G., & Queinnec, I. (2011). *Stability and stabilization of linear systems with saturating actuators*. Springer-Verlag London.

Wang, L. (2009). *Model predictive control system design and implementation using MATLAB*. Springer London.

Wang, L., & Xiao, F. (2010). Finite-time consensus problems for networks of dynamic agents. *IEEE Transactions on Automatic Control*, *55*(4), 950–955.

Weng, C., Feng, X., Sun, J., & Peng, H. (2016). State-of-health monitoring of lithium-ion battery modules and packs via incremental capacity peak tracking. *Applied Energy*, *180*, 360–368.

Wu, J., & Shi, Y. (2011). Consensus in multi-agent systems with random delays governed by a markov chain. *Systems & Control Letters*, *60*(10), 863–870.

Yang, T., Meng, Z., Dimarogonas, D. V., & Johansson, K. H. (2014). Global consensus for discrete-time multi-agent systems with input saturation constraints. *Automatica*, *50*(2), 499–506.

Yoo, S. J. (2013). Distributed adaptive containment control of uncertain nonlinear multi-agent systems in strict-feedback form. *Automatica*, *49*(7), 2145–2153.

Yu, W., Chen, G., & Cao, M. (2010). Distributed leader-follower flocking control for multi-agent dynamical systems with time-varying velocities. *Systems & Control Letters*, *59*(9), 543–552.

Yu, J., & Wang, L. (2010). Group consensus in multi-agent systems with switching topologies and communication delays. *Systems & Control Letters*, *59*(6), 340–348.

Yu, M., Yan, C., & Xie, D. (2017). Event-triggered control for couple-group multi-agent systems with logarithmic quantizers and communication delays. *Asian Journal of Control*, *19*(2), 681–691.

Yu, M., Yan, C., Xie, D., & Xie, G. (2016). Event-triggered tracking consensus with packet losses and time-varying delays. *IEEE/CAA Journal of Automatica Sinica*, *3*(2), 165–173.

Zheng, H., Negenborn, R. R., & Lodewijks, G. (2017). Fast ADMM for distributed model predictive control of cooperative waterborne AGVs. *IEEE Transactions on Control Systems Technology*, *25*(5), 1406–1413.

Zou, C., Manzie, C., Nešić, D., & Kallapur, A. G. (2016). Multi-time-scale observer design for state-of-charge and state-of-health of a lithium-ion battery. *Journal of Power Sources*, *335*, 121–130.